Chemical Engineering Journal 152 (2009) 307–314

Contents lists available at ScienceDirect

Chemical Engineering Journal

journal homepage: www.elsevier.com/locate/cej

Large-eddy simulations of particle sedimentation in a longitudinal sedimentation basin of a water treatment plant. Part I: Particle settling performance

M. Al-Sammarraee, A. Chan*, S.M. Salim, U.S. Mahabaleswar

Department of Chemical and Environmental Engineering, University of Nottingham (Malaysia Campus), Jalan Broga, 43500 Semenyih, Selangor Darul Ehsan, Malaysia

ARTICLE INFO

Article history:
Received 7 August 2008
Received in revised form 10 April 2009
Accepted 27 April 2009

Keywords:
Water treatment plant
Longitudinal sedimentation tank
Large-eddy simulations
Particle settling
Sedimentation

ABSTRACT

The process of particle sedimentation in a three-dimensional longitudinal basin in a water treatment plant is studied computationally. The fluid mixture mimics typical contaminated water in which the contaminants are represented by a spectrum of 13 different particle sizes. The processes of sedimentation of all classes of particles are simulated. The flow patterns, the particle settling velocities, the effectiveness of the particle removal from the stream and the particle concentrations distributions along the basin are estimated using large-eddy simulations (LES). Moreover the particles settling phenomenon and efficiency for different sizes of particles and the overall sedimentation efficiency of the basin are calculated.

Results show that longitudinal tanks are more efficient in dealing with larger particles compared to smaller particles in terms of settling. The influent is flushed downwards to the tank bottom. The flow then creates a large recirculation eddy near the sump area. Smaller recirculation regions, which are important to sedimentations, are also found near the entry and near the exit weir. Turbulence is generated near the inlet and outlet weir of the basin which also tends to inhibit settling. As a result, smaller particles tend to distribute more evenly in the basin while the larger particles settle quickly near the sump. The flow paths of the smaller particles also show that there is necessity in altering the geometries to enhance settling, especially near these turbulent regions. It also shows that there is a great deal of interactions with the sedimentation tank geometry which has significant improvements on the design aspects of these basins.

1. Introduction

Water supplied for public use must be potable from the standpoint of its chemical, physical and biological characteristics [1–4]. Drinking water should preferably be obtained from a source free from pollution or contaminants. The raw water normally available from surface water sources is, however, not directly suitable for drinking. The main objective of water treatment process is to produce safe and potable drinking water [1–5]. To such end, many water treatment processes have been developed and used for decades, such as coagulation–flocculation units, sedimentation basins, slow sand filtration, rapid sand filtration and disinfection units [1–4,6].

Sedimentation tanks are one of the most important components and the workhorses of any water purification plants. It is thus crucial for the sedimentation tank to operate at its full potential. It is not only the physico-chemical aspects of flocculation that is important. Hydraulics plays a prominent part [1–2,7]. Overdesign of sedimentation tank is common, leading not only to unnecessary capital expenditure, but also to water wastage in the form of excessive sludge. Improper and inadequate design cause overloading of filters, and lead to frequent backwashing, which in turn waste a significant percentage of treated water. Since treatment tanks tend to last a few decades, most do not incorporate the latest developments in technology to deal with these issues [1–5,8,9]. In this respect, good understanding of the various hydraulic processes within water treatment is essential for good design.

Sedimentation is a solid–liquid separation process, in which particles settle under the force of gravity. Particles with density greater than that of water deviate from the streamline of fluid flow by gravity and settle on the bottom of sedimentation tank [1–5,8,9]. At the same time these particles undergo various hydrodynamic and physical processes due to the shear forces in water flow which eventually affect the aggregation process and their removal efficiency [10–13]. Hence the sedimentation tank performance is strongly influenced by effects such as density driven flow, gravity sedimentation and flocculation and thickening. In turn the velocity and density patterns in tanks influence these processes and are therefore of great interest to design engineers [1–5,12,13].

* Corresponding author. Tel.: +60 3 89248144; fax: +60 3 89248017.
E-mail address: andy.chan@nottingham.edu.my (A. Chan).

1385-8947/$ – see front matter.
doi:10.1016/j.cej.2009.04.062

The primary performance indicator for sedimentation tanks is the fraction of the solids present in the raw water removed by the sedimentation step or sump. However this statistics is insufficient and can be misleading—an overdesigned tank will remove a large percentage without being really efficient. Therefore it is necessary to qualify it in terms of the design capacity [1–5,8,9].

Recently many research works had employed computational fluid dynamics (CFD) techniques to model the processes within different wastewater sedimentation tanks units in order to predict the fluid flow patterns and particle dispersions during each phase along these tanks. Larsen [14] first applied a CFD model to several secondary clarifiers. He demonstrated the presence of a pycnocline in a basin which causes the incoming fluid to sink to the tank bottom soon after entering. Shamber and Larock [15] used a finite volume method to solve the Navier–Stokes equations, the k–ε model and a solid concentration equation to model settling in secondary clarifiers. Long et al. [7] studied the flow dynamics in a secondary sedimentation tank and modelled the solid–liquid two-phase turbulent flow in the tank by a three-dimensional two-fluid model. Circular sedimentation tanks had been studied by Goula et al. [12] by employing CFD simulations to assess the effect of adding a vertical baffle at the feed section of a full-scale circular sedimentation tank for the improvement of solids settling in potable water treatment. Furthermore, Heath and Koh [13] incorporated a population balance model into the CFD code to model particle aggregation in solid–liquid separation systems. A two-dimensional circular clarifier has been modelled by McCorquodale and Zhou [16]. Their model consists of two parts: a flow model providing the velocity and turbulent viscosity field (unsteady, turbulent, density stratified flow) and a suspended sediment transport model for determining the particle concentration field. CFD simulations were also used to analyse the sediment transport for multiple sediment sizes to estimate the efficiency of solids removal in a raceway, which can provide information on the distribution and flow of particles and on the proportion of the solids that settle [17]. Information as such can be used to estimate the efficiency of the whole process.

However, in spite of the mentioned works, very little had been done to study the longitudinal sedimentation basin concerning water treatment in terms of the settling of suspended solids in these units, the distribution of velocity and suspended solids, the turbulent diffusion of suspended solids and most importantly the settling efficiency of these units. This information is important in design to increase the efficiency of particles removal which is a crucial aspect of the longitudinal sedimentation basin design. Longitudinal sedimentation basin play a vital role in water treatment plants especially in Europe as these units offer higher surface rates, less maintenance and better quality [8]. Longitudinal sedimentation basins are horizontal rectangular basins with a high ratio of length to width (4:1). This helps in increasing the resident time for water flow in sedimentation basin which increases the settling time for the suspended particles [1–5]. Longitudinal basins are also easier to design, build and operate compared to circular tanks.

The objectives of this research are two-fold. We would like to investigate numerically the sedimentation process of a real three-dimensional longitudinal sedimentation basin. The flow patterns, velocity profiles, turbulence, and particles distribution would be investigated. In this tank, the size of the particles is classified into 13 different size and the settling phenomenon and efficiency for each particle class and for all classes together are estimated using a two-phase model. Moreover we would like to study the use the LES model in the flow and sedimentation modelling.

Fig. 1. Longitudinal sedimentation basin in the water treatment plant.

2. Computational fluid dynamics modelling

The longitudinal sedimentation basin being investigated is a real tank as in Fig. 1. Due to contractual reasons, the tank will not be identified and its location is undisclosable. While the k–ε model is probably the commonest turbulence model in research and practical applications, it is well-known that severe inaccuracies will arise near zones of strong shear or when the Reynolds number is low or moderate [18]. Ironically such situations are very important in the sedimentation process, as sedimentation takes place near the wall or sump area and that motions of individual particles are dictated by the fine structures of the flow, which could not be adequately resolved by k–ε model. Moreover the local Reynolds number of the flow near the particle during sedimentations is inevitably small. All these suggest the consideration of LES in studying sedimentations, leaving aside temporarily the issue of computational cost.

2.1. Large-eddy simulations

The governing equations employed for LES are obtained by filtering the time-dependent Navier–Stokes equations in the physical space [19,20].

The filtered Navier–Stokes equations are,

$$\frac{\partial \overline{u_i}}{\partial x_i} = 0, \tag{1}$$

$$\frac{\partial \overline{u_i}}{\partial t} + u_j \frac{\partial \overline{u_i}}{\partial x_j} = -\frac{1}{\rho}\frac{\partial \bar{p}}{\partial x_i} + \upsilon \frac{\partial^2 \overline{u_i}}{\partial x_j^2} - \frac{\partial \tau_{ij}^{\gamma}}{\partial x_j} - gk, \tag{2}$$

where $\overline{u_i}$ is the filtered velocity component in the ith direction, $\bar{p}$ the filtered pressure, ρ the density of the fluid, υ the kinematic viscosity of the fluid, g the gravitational acceleration directing vertically downwards taken as the k-direction, and τ_{ij}^{γ} is the anisotropic residual stress tensor. Closure of the problems is achieved using the static Smagorinsky model [19,20]

$$\tau_{ij}^{\gamma} = 2^{3/2}(C_s \Delta \overline{S_{ij}})^2, \tag{3}$$

where C_s is the Smagorinsky constant (~ 0.17), Δ is the filter-size and S_{ij} is the rate of strain tensor.

2.2. The grid and the boundary conditions

The geometry had been constructed for the longitudinal sedimentation tank with the dimensions illustrated in Table 1, following the real dimensions.

The tank in consideration and its computational grid is shown in Fig. 2. The tank bottom has a bottom slope of 4°. The inlet flow rate is 180 m^3/h with a pressure outlet boundary condition imposed at

Table 1
Dimension of sedimentation tank.

	Length/m	Width/m	Depth/m	Number
Tank	20	3	1–2.5	
Outlet weirs	2.5	0.6	0.4	3

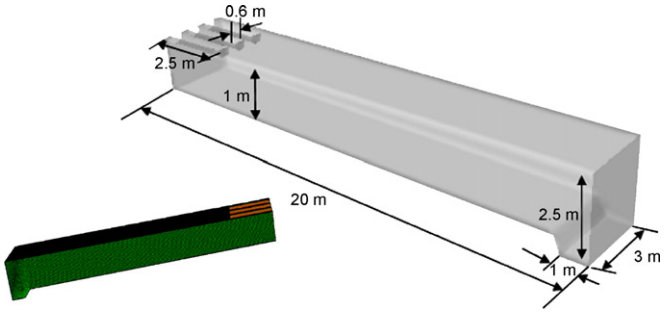

Fig. 2. The geometry and the computational mesh of the longitudinal sedimentation tank.

the weir end, using real data from the tank. The tank is considered to be full of water devoid of a free surface.

2.3. Particles

The inlet flow consists of two phases: the primary phase is water and the secondary phase is particles. The particles are divided into 13 classes based on the diameter of the particle. The classification is based on raw water data measured using laser diffraction technique [12] as illustrated in Table 2. The simulation process had been made for each particle class as a secondary phase.

The mass flow rate in kg s^{-1} of each class of particles had been estimated. The particle spectrum with their corresponding mass fraction that enters the sedimentation basin is shown in Fig. 3, The particle concentration at the entrant of the sedimentation basin is 1000 mg/l, the corresponding water inlet velocity (volumetric flow rate over sedimentation basin cross-sectional area perpendicular to the flow) equals to 0.0024 m s^{-1} along the basin. The effective density of the particles and water is 1066 kg m^{-3} and 998.2 kg m^{-3}, respectively. The condition of slip velocity between the two phases had been neglected since there is only a minute difference between the densities of the two phases [7]. In longitudinal sedimentation tank sludge will be drawn intermittently from the sump section, and thus no consideration for the presence of sludge is made [7,21].

To model the two-phase flows, a Lagrangian mixture approach is taken using the discrete phase model. This approach is taken

Table 2
Particle size classification.

Particles class	Mean particle diameter/μm	Mass fraction	Mass flow rate/kg s^{-1}
1	20	0.025	0.00125
2	50	0.027	0.00135
3	80	0.039	0.00195
4	120	0.066	0.0033
5	170	0.095	0.00475
6	200	0.115	0.00575
7	250	0.126	0.0063
8	350	0.124	0.0062
9	450	0.113	0.00565
10	550	0.101	0.00505
11	650	0.077	0.00385
12	750	0.057	0.00285
13	850	0.04	0.002
	Total	1.00	0.05025

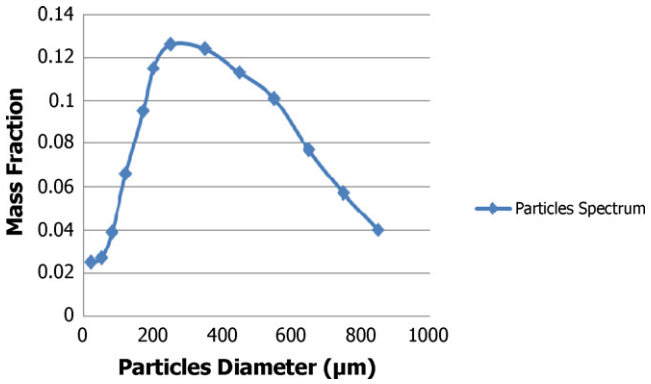

Fig. 3. Particles spectrum at the sedimentation tank influent.

based on Goula et al. [12] where the Lagrangian model is good when particle volume fraction is small and that the presence of the particles does not affect the flow. This means the fluid mechanics problem is thus decoupled and that the hydrodynamics of the tank can be solved first without the particles. The mixture model is a simplified multiphase model that can be used to model multiphase flows where the phases move at different velocities, but assuming local equilibrium exists over short spatial length scales. The mixture model simulates phases (fluid or particulate) by solving the momentum, continuity, and energy equations for the mixture, the volume fraction equations for the secondary phases, and algebraic expressions for the relative velocities. Particles are injected after the hydrodynamics of the tank is solved. Superposition principle is invoked to estimate the total sedimentation efficiency. In all our cases, the volume fraction remains small and thus the Lagrangian model is feasible [22].

The dispersion of the particles due to turbulence is modelled using a stochastic discrete particle approach as in Goula et al. [12] after the filtered velocities are obtained from the hydrodynamic calculations. The trajectory of individual particles are integrated using the instantaneous filtered velocity components along the particle trajectory.

2.4. Numerical simulation

The code being used is FLUENT 6.3. Typical time for convergence to an acceptable level of accuracy is around 1 day on a 4-node parallel personal computer. The segregated unsteady solution algorithm with bounded central differencing is selected to solve the continuity, and momentum equations. Second-order upwind is used to calculate the volume fraction for the particle concentration. For the flow near the wall the choice of the standard wall function is incorporated into the model because the fluid velocity is low (0.0024 m s^{-1}). This makes the walls of the sedimentation tank comparatively smooth with a large viscous sublayer [12].

The computations were performed in three-dimensional to capture the full picture of turbulence, especially when the Reynolds number is so high. Goula et al. [12] studied a circular tank using a 2D k–ω model for a circular tank but it is believed that the turbulence in a rectangular tank is more chaotic and thus 3D simulations are preferred. The 3D code is used to study the problem of Goula et al. [12] and good agreements have been achieved with their 2D data, as far as the bulk velocity is concerned. Obviously small differences in turbulence and circulations patterns are observed but by and large the flow patterns are close. Moreover a subsequent experimental measurement of the particle concentration was performed in the real tank at the effluent to compare the experimental and computational data as in Fig. 4. Very satisfactory agreement is achieved.

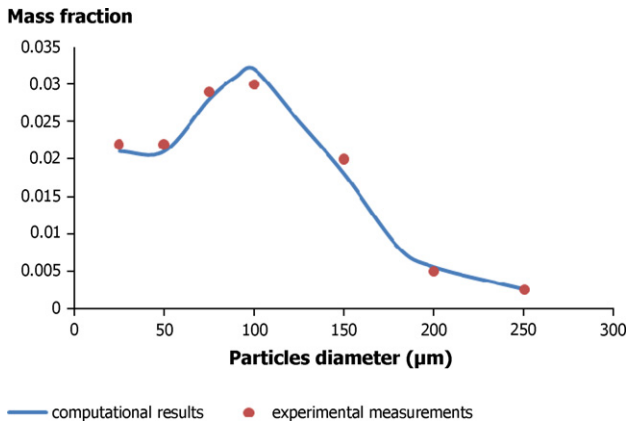

Fig. 4. Experimental and computational results of mass fraction of particles at the exit weir.

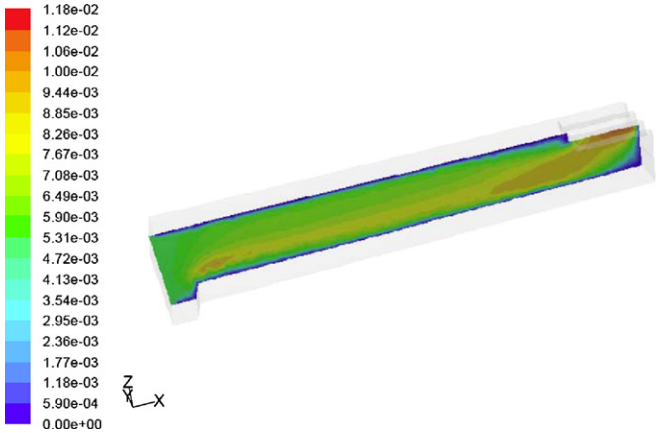

Fig. 6. Velocity contours of particles using the LES for Class 1 particles.

A grid-dependency study was performed to determine the best compromise between accuracy, stability and computational cost. A few grids (0.1, 0.5, 1, 2.5 and 5 million cells) were considered and obviously the results from different grids are slightly different. However the difference is actually quite insignificant for all the grids. As a matter of fact, all the grids give very similar results even with the coarse grid. The final mesh comprises of 2.5 millions tetrahedral cells, meaning a typical cell is a maximum of 0.05 m in the far-field, resolving towards 0.0005 m near the walls and inlet.

LES was chosen as the turbulence scheme because we want to look at the large turbulence structures that affect sedimentation and settling. PISO was used to enhance convergence, and the predetermined residual for convergence was set to 1×10^{-6}.

3. Results and discussions

3.1. Flow pattern

We first study the flow patterns inside the tank for different particle size. The mid-plane located inside the sedimentation tank is used to analyse the particle velocities, the mixture turbulence contour and the particle settling velocity contours and the particle settling velocities in vertical direction along the basin.

An initial comparison was made between the use of the k–ε model and the LES model for the preliminary studies as shown in Figs. 5 and 6. In general, little differences are shown between the two models in terms of velocity, turbulence, and particle settling velocity and most importantly the estimated settling efficiencies, especially in the bulk part of the basin. However, closer examination shows that the k–ε model fails to capture the flow properly in areas of strong turbulence and shear, for example at the inlet, the exit and near the bottom. Moreover, the shear zones and near wall regions shows that LES is able to resolve the velocities more accurately. It is noted that the k–ε model is dedicated for high Reynolds flow which is inaccurate in simulating sedimentation basin with low velocity flow (Reynolds number of the flow is around 10 based on the basin height). This is further confirmed with the validation exercise with the experimental data where the LES simulations obtain much better agreements. As expected, the k–ε model over-predicts the turbulence at the shear zone as in the case of flow past bluff bodies [18]. The k–ε model also fails to resolve flow structures around the particles and near the bottom with sufficient accuracies. After all LES is designed to model eddy motions or strong shear which is prominent in the situation, and thus LES is a good computational model for the study [21–23]. The improvement in accuracy is also justified considering the acceptable increase in computational cost in using LES.

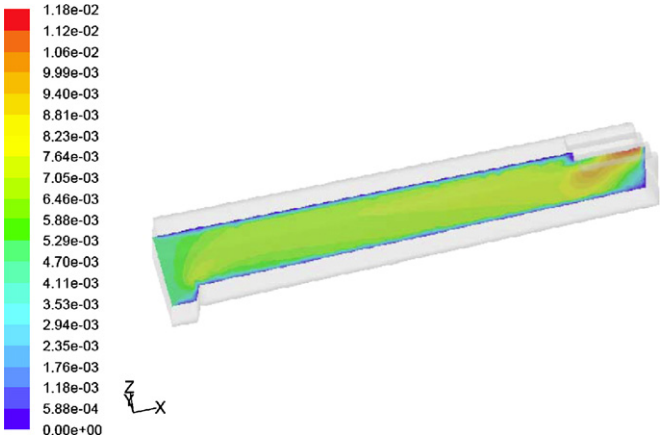

Fig. 5. Velocity contours of particles using the k–ε model for Class 1 particles.

We now discuss the response of each of the particles class in sedimentation. As expected, the settling efficiency decreases as particle size decreases because it is much more difficult to settle small particles. Larger particles settle quickly due to their masses and their inertia towards turbulence. As an illustration, we show the behaviour of different sized particles in the tank. The displayed simulations refer to particles of selected small-size Class 1 (20 μm), medium-size Class 4 (120 μm), and large-size Class 13 (850 μm) (Table 2).

As expected, it is difficult for the small-size particles to settle and hence it can be seen from Figs. 7 and 8 that the small particles are dispersed almost evenly along the basin. A small fraction of the particles is able to settle near the entry trough due to turbulence while the rest distributes evenly along the basin. Fig. 9 shows the velocity of the flow and it can be seen that the turbulence of the system is not strong enough to trap the particles through the small eddies. As observed in Goula et al. [12] and also McCorquodale and Zhou [16], the influent is flushed very quickly downwards to the tank bottom at the inlet. The flow then creates a large recirculation eddy near the sump area. Smaller recirculation regions, which are important to sedimentations, are also found near the entry and near the exit weir. Turbulence generated by the lighter particles is small throughout because of its relatively small fluctuations and turbulent kinetic energy. This is further substantiated from the settling velocity diagram of Fig. 10, showing the very small settling velocity which enhances larger dispersion but discourage sedimentation.

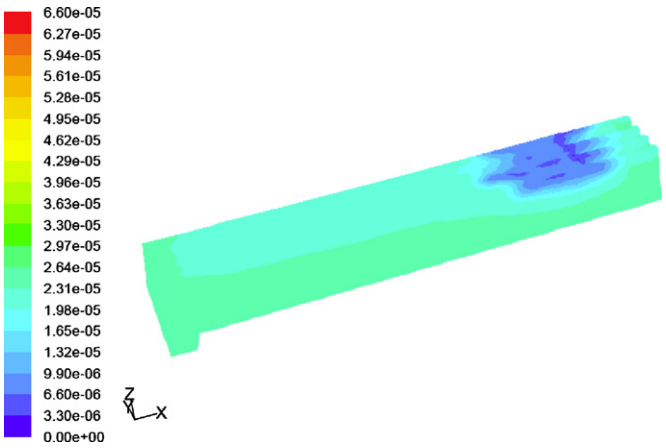

Fig. 7. Volume fraction contour of small-size particles (Class 1) top view.

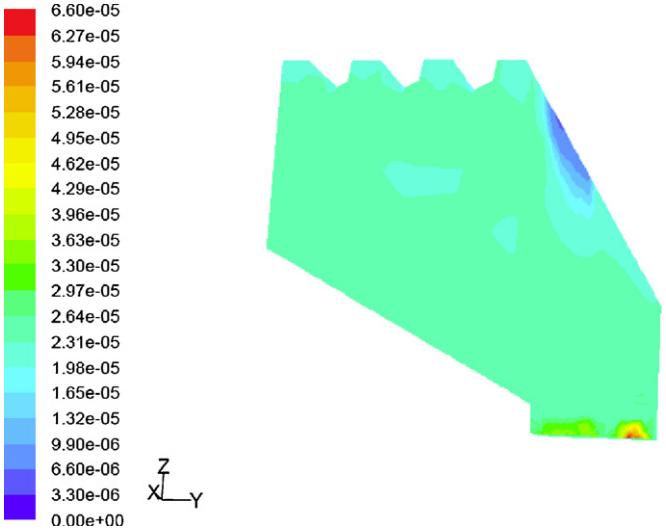

Fig. 8. Volume fraction contour of small-size particles (Class 1) bottom view.

Fig. 10 shows the settling velocity along the basin. The location of these measurements follow that of Micale et al. [24], in which a diagonal line is drawn from the bottom near the basin entrance towards the weir at the exit. This will measure the settling velocity along the height and length of the basin simultaneously. Near the entrant, the settling velocity is close to zero, due to the balances

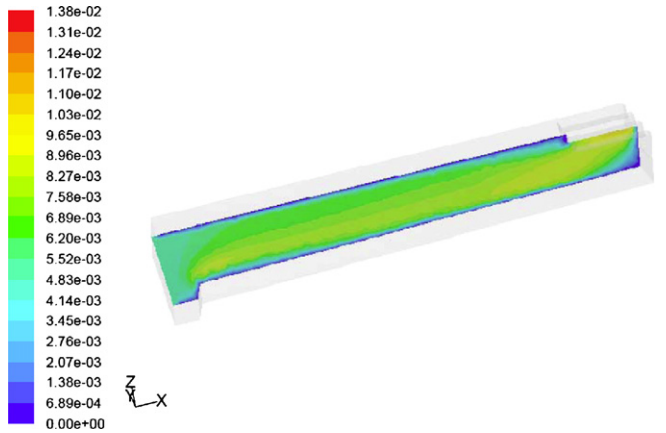

Fig. 9. Velocity magnitude contour of small-size particles (Class 1).

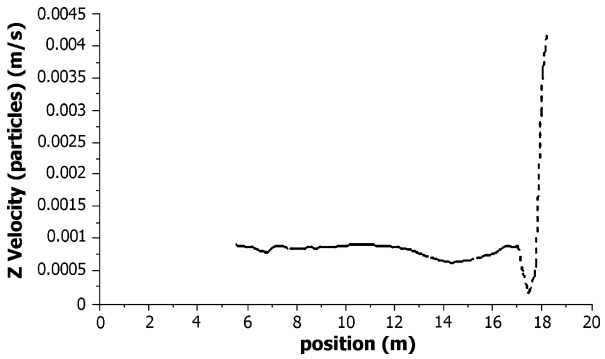

Fig. 10. Particle settling velocity for small-size particles along the basin (Class 1).

of inertial forces with buoyancy and upthrust. Moreover, near the entrance, measurements are taken very close to the bottom, and it is expected that the settling velocity to be very small. Essentially, the particles near the entrant oscillate around the turbulent structures. In fact except for the small region near the exit weir, the settling velocities of the particles remain evenly small along the basin. The exit surge is simply promoted by the exit flow. This agreed with Micale et al. [24] who showed that in the case of millimetre or sub-millimetre particles falling in water the effect of free-stream turbulence is to increase particles drag force and therefore decrease their settling velocity.

There is good agreement with the trend of the experiment data obtained by Micale et al. [24] when they estimated the terminal velocity of particles based on measurements made in water with the settling velocities illustrated in Figs. 9, 14 and 19 for the Classes 1, 4, and 13 (Table 2). Marchioli et al. [23] observed in their direct numerical simulation (DNS) that in the case of small particles gravity has little effect on their average settling velocity, which tends to remain smaller than the average turbulent fluctuating velocities.

Fig. 11 shows the volume fraction of medium-sized particles (Class 4). It is immediately obvious from the bottom view that the medium-size particles settle much quickly than Class 1 particles, though the settling is still near to the weir end, rather than the entry trough. This can be explained in Fig. 12 that the velocities are large near the end of the basin, thus carrying a lot of particles around that proximity.

Fig. 13 shows the turbulence intensity along the basin. This is to show where the small-scale eddies are located. These small eddies are responsible to trap particles and help them settle along the basin. It is clear from the figure that these eddies are located both near the inlet trough and the exit weir, corresponding approx-

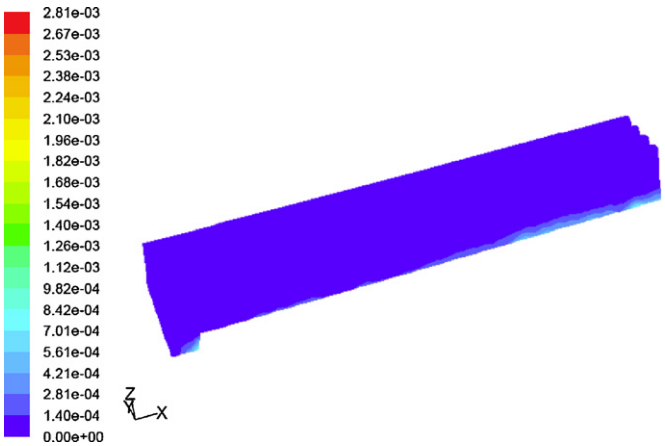

Fig. 11. Volume fraction contour of medium-size particles (Class 4).

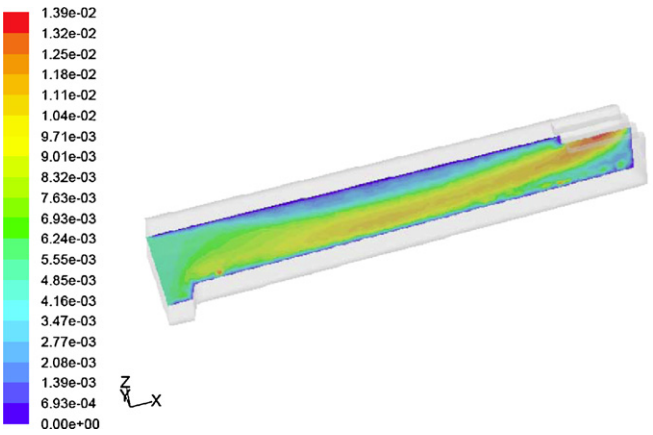

Fig. 12. Velocity magnitude contour of medium-size particles (Class 4).

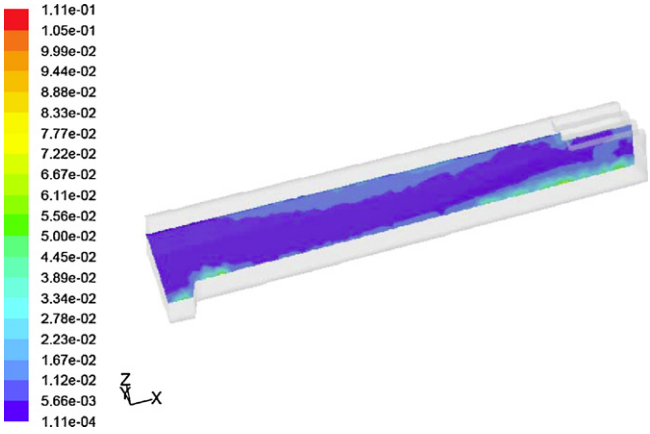

Fig. 13. Turbulence contour of mixture for medium-size particles (Class 4).

imately to where settling of medium-size particles are. This is further substantiated in Fig. 14, the particle settling velocity for the medium-size particles. The trend of the settling velocity of Fig. 14 is similar to Class 1 particle. The settling velocity is insignificantly small near the basin entrant, due to measurement taken near the bottom and shoots up near the weir end.

Larger-size particles are expected to settle quickly along the basin because of its mass and inertia. As a matter of fact from Table 3, 100% settling is achieved for particles Class 8. Fig. 15 shows that the large-size particles (Class 13) basically settle all inside the inlet trough. Fig. 16 shows the velocity contour of the large-size particles and it can be seen that the particles basically concentrate near

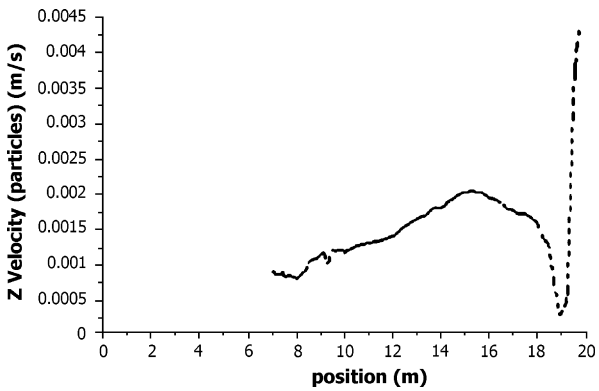

Fig. 14. Medium-size particle settling velocity along basin (Class 4).

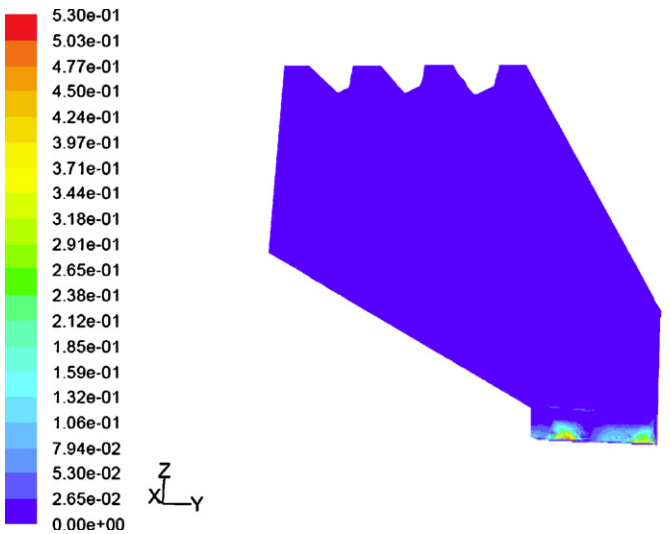

Fig. 15. Volume fraction contour of large-size particles (Class 13) at basin bottom.

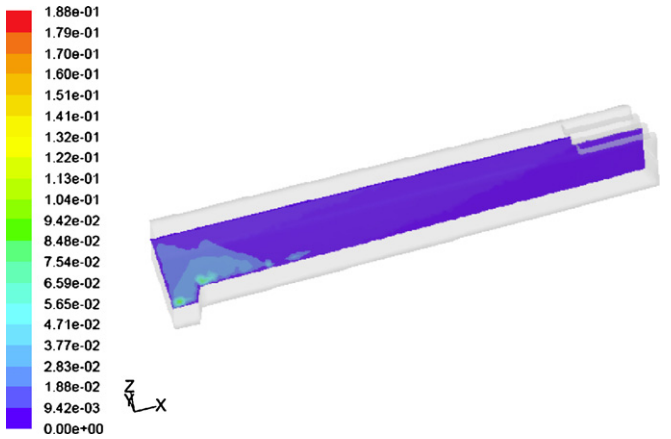

Fig. 16. Velocity magnitude contour of large-size particles (Class 13).

the inlet, implying that all the particles tend to settle quickly near the inlet trough because of their weight. From Figs. 17 and 18, the velocity vector plots of individual particles and the turbulence plot, it is clear that there are hardly any particles away from the inlet.

Fig. 19 shows these particles settling velocity along the basin, and again it is obvious that the larger particles tend to settle at large velocity along the basin.

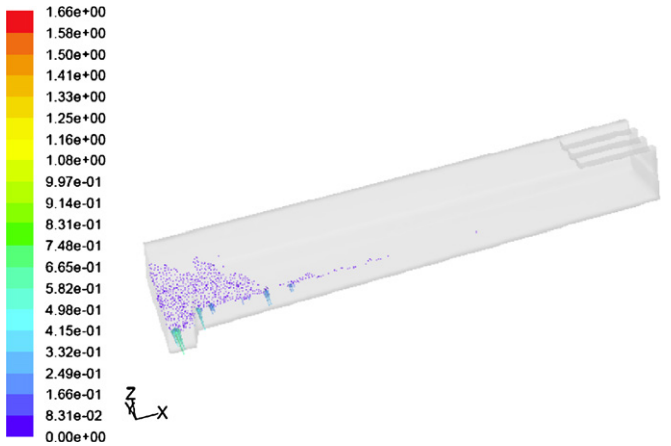

Fig. 17. Velocity vectors of large-size particles (Class 13).

Table 3
Settling of different class of particles in sedimentation tank.

Particles class	Mean particles diameter/μm	Mass fraction	Particles mass flow rate/kg s^{-1}	Settling efficiency/%
1	20	0.025	0.00125	16
2	50	0.027	0.00135	19
3	80	0.039	0.00195	24
4	120	0.066	0.0033	49
5	170	0.095	0.00475	87
6	200	0.115	0.00575	94
7	250	0.126	0.0063	97
8	350	0.124	0.0062	100
9	450	0.113	0.00565	100
10	550	0.101	0.00505	100
11	650	0.077	0.00385	100
12	750	0.057	0.00285	100
13	850	0.04	0.002	100
	Total	1.00	0.05025	87.144

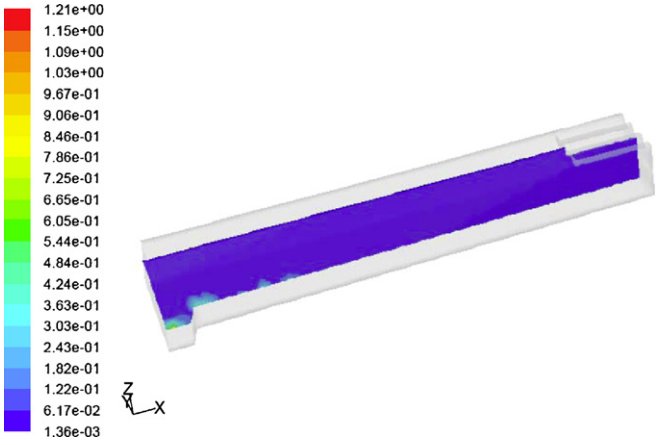

Fig. 18. Turbulence contour of mixture of large-size particles (Class 13).

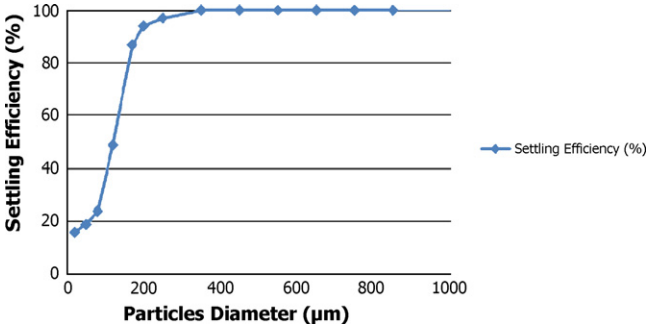

Fig. 20. Particles settling efficiency.

3.2. Particles settling efficiency

The most important performance criterion for the sedimentation basin is the settling efficiency. Particles settling efficiency for each individual class has been estimated by computing the mass flux of the particles in the inlet and outlet streams, respectively, and is shown in Table 3 and Fig. 20. The total particles settling efficiency for the longitudinal sedimentation basin is calculated by multiplying each particle mass fraction with its corresponding settling efficiency divided by the total mass fraction of particles as shown in Table 3 and Fig. 20.

The results obtained for total particles settling efficiency are similar to the work done by Goula et al. [12] for a 2D circular clarifier in water treatment plant which yields a total settling efficiency of 85%. In contrast the settling efficiency for each particle class are even better compared to the simulation work done by Huggins et al. [17] on the solids removal in a raceway with six different particles sizes. The particles spectrum in the inlet (influent) and outlet of the sedimentation tank (effluent) is illustrated in Fig. 21. From the figure, it is very clear that the basin has effectively removed all medium to large-size particles and shrinking the particle spectrum, in terms of number and in terms of spectrum size. It is understandable that sedimentation is easier for the large-size particles compared to the lighter ones due to its mass.

In general, the impact of gravity on the motion of small particles is weak, whereas in the case of large particles, velocity correlations along the particle trajectories tend to decrease due to the crossing-trajectory effect and particle motion becomes disengaged from fluid

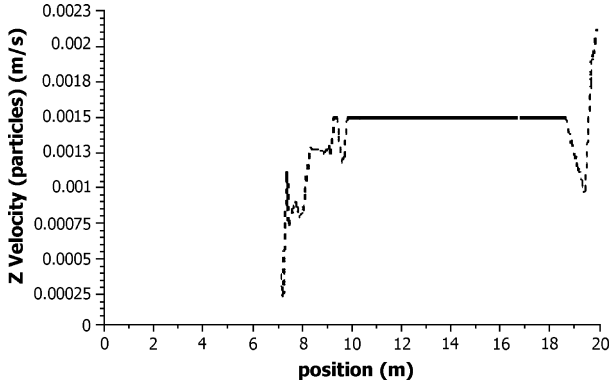

Fig. 19. Particle settling velocity for large-size particles along basin (Class 13).

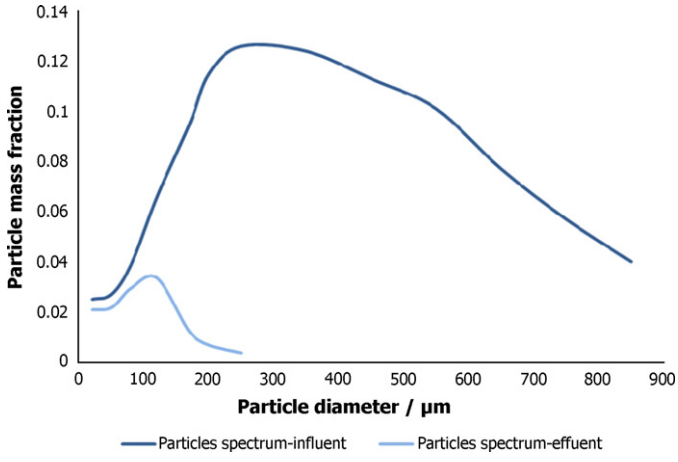

Fig. 21. Particles spectrum in the sedimentation tank.

turbulence. In our case this happens with large particles of Class 13 (Figs. 16 and 17), where it is shown that the particles decrease in velocities until it reaches the bottom of the tank and die out very close to the sedimentation tank entrance. A similar situation occurs for the volume fraction of these particles (Fig. 15) as opposed to the lighter particles (Classes 1 and 4) illustrated in Figs. 7 and 11.

Particles velocities show little difference near the entrance, and also at the outlet weir near the wall region. This happened due to sedimentation tank geometry with a sloped bottom, the flow coming from the entrance faces a narrow area in the end of the sump section and this leads to particles accelerating near the exit. Furthermore an increase in particle velocities near the outlet weir is common; the velocities extend backward into the settling zone causing particles to be drawn into the outlet weir of the sedimentation tank.

From Figs. 13 and 18, turbulence is typically generated close to the entrance and the outlet weir. Matko et al. [21] found that in sedimentation tanks, even though the mean flow velocities are relatively low compared to other processes, the Reynolds number is still high enough to cause turbulent flow. In fact turbulent flow in clarifiers is caused by mixing of the influent with the flow in the tank and the impact of the flow on the solid boundaries. Moreover Krepper et al. [25] found that larger objects are disintegrated under the influence of the shear stresses and turbulence from the surrounding liquid. The turbulent wake of the larger particle agglomerations causes breakages that result in the generation of finer particle fractions which is difficult to settle.

4. Conclusions

In this research a three-dimensional computational study is conducted for a longitudinal sedimentation basin in a water treatment plant using LES turbulence models. LES is considered a good model as it can accurately resolve the small-scale flow patterns around the sedimenting particles, which is otherwise unresolvable using conventional k–ε model. A comparison between LES and k–ε and good conclusions about the use of LES has been made.

The fluid mixture mimics typical contaminated water in which the contaminants are represented by a spectrum of 13 different particle sizes. The flow patterns, the particle settling velocities, the particle settling efficiency, volume fraction, and turbulence intensities along the sedimentation basin are computed using LES and a multiphase model. The overall sedimentation efficiency of the basin for all the cases are all calculated.

Results show that longitudinal tanks are more efficient in dealing with larger particles compared to smaller particles in terms of settling. The influent is flushed downwards to the tank bottom. The flow then creates a large recirculation eddy near the sump area. Turbulence is generated near the inlet and outlet weir of the basin which also tends to inhibit settling. As a result, smaller particles tend to distribute more evenly in the basin while the larger particles settle quickly near the sump.

The inlet and effluent particle spectrum are thus estimated by calculating the particle settling efficiency for the 13 classes of particles and the total settling efficiency of the longitudinal sedimentation basin. Comparisons had been made for the obtained results with the previous works and experimental data and showed good agreements.

From physical reasoning, it is more difficult for smaller and lighter particles to settle and they are dispersed more evenly around the tank, whereas heavier particles tend to settle quickly near the sump. This model predicts the distribution and the concentrations of particles along the sedimentation basin which are very important factors in designing these basins. This part of the work shows that longitudinal sedimentation basins are good, simple and effective devices to settle solid particles.

This work is the first in a series conducted to study and improve the performance of a real sedimentation tank. This part of the study is devoted to understand the hydrodynamics of the tank, which would lead to devising improvement of its performance. Part Two of this series is devoted to devise strategies to improve the performance of the sedimentation tank according to results of this study. Results of this work will be presented in a subsequent work.

Acknowledgement

The authors appreciate the important comments by the reviewers, with which the authors have made significant improvements on the work.

References

[1] M.L. Davis, D.A. Cornwell, Introduction to Environmental Engineering 3/e, McGraw-Hill, 1988.
[2] G. Kiely, Environmental Engineering, McGraw-Hill, 1998.
[3] S.H. Peavey, R.D. Rowe, G. Tchobanoglous, Environmental Engineering, McGraw-Hill, 1985.
[4] World Health Organization, Guidelines for Drinking water Quality 3/e, IWA Publishing, 2004.
[5] World Health Organization, Water Treatment and Pathogen Control, IWA Publishing, 2004.
[6] J.E. Ebeling, P.L. Sibrell, S.R. Ogden, S.T. Summerfelt, Evaluation of chemical coagulation/flocculation aids for the removal of suspended solids and phosphorus from intensive recirculating aquaculture effluent discharge, Aquacult. Eng. 29 (2003) 23–42.
[7] F. Long, N. Xu, X. Ke, H. Shi, Numerical simulation of secondary sedimentation tank for urban wastewater, J. Chin. Inst. Chem. Eng. 38 (2007) 425–433.
[8] D.G. Stevenson, Water Treatment Unit Process, Imperial College Press, 1997.
[9] J.M. Hammer, Water and Wastewater Technology 5/e, Prentice Hall, 2005.
[10] L. Wang, D.L. Marchisio, R.D. Vigil, R.O. Fox, CFD simulation of aggregation and breakage processes in laminar Taylor–Couette flow, J. Colloid Interface Sci. 282 (2005) 380–396.
[11] J. Kim, T.A. Kramer, Improved orthokinetic coagulation model for fractal colloids: aggregation and breakup, Chem. Eng. Sci. 61 (2006) 45–53.
[12] A.M. Goula, M. Kostoglou, T.D. Karapantsios, A.I. Zouboulis, A CFD methodology for the design of sedimentation tanks in potable water treatment case study: the influence of a feed flow control baffle, Chem. Eng. J. 140 (2008) 110–121.
[13] A.R. Heath, P.T.L. Koh, Combined population balance and CFD modeling of particle aggregation by polymeric flocculant, in: Proc. Third Int. Conf. CFD Miner. Process Ind., 2003, pp. 339–344.
[14] P. Larsen, On the hydraulics of rectangular settling basins, Report No. 1001, Department of Water Research Engineering, Lund Institute of Technology, 1977.
[15] D.R. Shamber, B.E. Larock, Numerical analysis of flow in sedimentation basins, J. Hydraul. Div. 107 (HY5) (1981) 575–591.
[16] J.A. McCorquodale, S. Zhou, Effects of hydraulic and solids loading on clarifier performance, J. Hydraul. Res. 31 (1993) 461–477.
[17] D.L. Huggins, R.H. Piedrahita, T. Rumsey, Analysis of sediment transport modeling using computational fluid dynamics (CFD) for aquaculture raceways, Aquacult. Eng. 31 (2004) 277–293.
[18] S. Murakami, Comparison of various turbulence models applied to a bluff body, J. Wind Eng. Ind. Aerodyn. 46/47 (1993) 21–36.
[19] S.B. Pope, Turbulent Flows, Cambridge University Press, 2003.
[20] D.C. Wilcox, Turbulence Modeling for CFD 2/e, Birmingham Press, 2004.
[21] T. Matko, N. Fawcett, A. Sharp, T. Stephenson, Recent progress in the numerical modeling of wastewater sedimentation tanks, J. Inst. Chem. Eng. 74 (1996) 246–258.
[22] B. de Clercq, P.A. Vanrolleghem, Computational fluid dynamics in wastewater treatment, Med. Fac. Landb. Toegep. Biol. Wet. 67 (2002) 15–19.
[23] C. Marchioli, M. Picciotto, A. Soldati, Influence of gravity and lift on particle velocity statistics and transfer rates in turbulent vertical channel flow, Int. J. Multiphase Flow 33 (2007) 227–251.
[24] G. Micale, G. Montante, F. Grisafi, A. Brucato, J. Godfrey, CFD simulation of particle distribution in stirred vessels, J. Inst. Chem. Engrs. 78 Part A (2000) 435–444.
[25] E. Krepper, G.C. Glover, A. Grahn, F.P. Weiss, S. Alt, R. Hampel, W. Kastner, A. Kratzsch, A. Seeliger, Numerical and experimental investigations for insulation particle transport phenomena in water flow, Ann. Nucl. Energy 35 (2008) 1564–1579.